RESEARCH PAPER

Epigenetics 6:2, 1-11; February 2011; © 2011 Landes Bioscience

Epigenetic quantification of tumor-infiltrating T-lymphocytes

Jalid Sehouli,[1,†] Christoph Loddenkemper,[2,†] Tatjana Cornu,[3,†] Tim Schwachula,[3,†] Ulrich Hoffmüller,[3] Andreas Grützkau,[4] Philipp Lohneis,[5] Thorsten Dickhaus,[6] Jörn Gröne,[7] Martin Kruschewski,[7] Alexander Mustea,[8] Ivana Turbachova,[3] Udo Baron[3] and Sven Olek[3,*]

[1]Klinik für Frauenheilkunde; Charité-Universitätsmedizin; Campus Virchow; Berlin, Germany; [2]Institut für Allgemeine Pathologie; Technische Universität München; [3]Epiontis; Berlin, Germany; [4]Deutsches Rheumaforschungszentrum Berlin; [5]Institut für Pathologie; [6]Humboldt Universität Berlin; Mathematik; and [7]Chirurgische Klinik I; Charité-Universitätsmedizin; Campus Benjamin Franklin, Berlin, Germany; [8]Klinik für Frauenheilkunde, Universität Greifswald, Greifswald, Germany

[†]These authors contributed equally to this work.

Key words: tumor immunology, regulatory T cells, T-lymphocytes, epigenetic immunophenotyping, DNA methylation

Abbreviations: Amp, amplicon; CD3D/G, T-cell surface glycoprotein CD3 delta/gamma chains; FOXP3, forkhead box protein P3; OT, healthy ovarian tissue; OvCa, ovarian cancer tissue; BT, healthy bronchial tissue; BCa, bronchial cancer tissue; CT, healthy colorectal tissue; CRC, colorectal cancer tissue; TSDR, treg specifically demethylated region; oTL, overall T-lymphocytes

The immune system plays a pivotal role in tumor establishment. However, the role of T-lymphocytes within the tumor microenvironment as major cellular component of the adaptive effector immune response and their counterpart, regulatory T-cells (Treg), responsible for suppressive immune modulation, is not completely understood. This is partly due to the lack of reliable technical solutions for specific cell quantification in solid tissues. Previous reports indicated that epigenetic marks of immune cells, such as the Treg specifically demethylated region (TSDR) within the FOXP3 gene, may be exploited as robust analytical tool for Treg-quantification. Here, we expand the concept of epigenetic immunophenotyping to overall T-lymphocytes (oTL). This tool allows cell quantification with at least equivalent precision to FACS and is adoptable for analysis of blood and solid tissues. Based on this method, we analyze the frequency of Treg, oTL and their ratio in independent cohorts of healthy and tumorous ovarian, colorectal and bronchial tissues with 616 partly donor-matched samples. We find a shift of the median ratio of Treg-to-oTL from 3–8% in healthy tissue to 18–25% in all tumor entities. Epigenetically determined oTL frequencies correlate with the outcome of colorectal and ovarian cancers. Together, our data show that the composition of immune cells in tumor microenvironments can be quantitatively assessed by epigenetic measurements. This composition is disturbed in solid tumors, indicating a fundamental mechanism of tumor immune evasion. Epigenetic quantification of T-lymphocytes serves as independent clinical parameter for outcome prognosis.

Introduction

Establishment of malignant tumors depends on favorable growth kinetics of tumor cells[1] and their strategies to escape from immune surveillance.[2] Until recently, therapies focused on eradication of malignant cells, which is mostly unable to cure later stage disease. The immune system was recognized as additional target, due to its ambiguous role in exhibiting host protection on one, and facilitating tumor growth on the other hand.[3] Antigen-specific host protection is achieved via the adaptive immune system, consisting of B- and T-lymphocytes. The latter are collectively defined by expression of the T-cell receptor (TCR) complex including the T-cell surface glycoprotein CD3.[4] Tumor cells express specific antigens, thus becoming targets for T-cell-mediated immune responses. Mouse experiments confirm a role of T-cells in cancer immune surveillance[2,5,6] and tumor-infiltrating overall T-lymphocytes (oTL) inhibit tumor growth in colorectal and ovarian cancers.[7-10] Also, increased CD3 mRNA levels in the tumor correlate with improved outcome.[11] The function of regulatory T-cells (Treg) is converse to the role of effector T-lymphocytes. They control effector T-cell responses and mediate immunological tolerance referring to the ability of the adaptive immune system to spare certain antigens from immunological attack. Treg are identified by expression of CD3, CD4, CD25 and FOXP3. Further markers, including CD127, CTLA4, GITR, CD45RA or CD103, are used for Treg isolation and characterization in order to increase specificity.[12-16] It was proposed that tumor growth is facilitated by elevated levels

*Correspondence to: Sven Olek; Email: sven.olek@epiontis.com
Submitted: 07/13/10; Accepted: 09/25/10
Previously published online: www.landesbioscience.com/journals/epigenetics/article/13755

of $CD4^+CD25^+$ assumed Treg, since increased Treg-numbers have been observed in hepatocellular, gastric and esophageal cancers.[17,18] Reports have also associated lower levels of intratumoral $CD4^+CD25^+FOXP3^+$ cells with better outcome in ovarian cancer[19] and lower risk of recurrence in stage I non-small cell lung cancer patients.[20] The persuasive thought that the number of tumor-infiltrating Treg inversely correlate with patient prognosis is supported by data showing abrogation of immunological unresponsiveness in murine tumor models upon removal of $CD4^+CD25^+$ T-cells.[21] However, other studies do not confirm a prognostic value.[22] Since all known Treg-expression markers are displayed by activated effector T-cells, quantification of Treg is blurred[23-25] and it remains unclear if elevated $CD25^+CD4^+$ cell counts in tumors reflect, at least partly, transiently FOXP3 expressing $CD25^+$ effector T-cells rather than natural Treg.[26,27] This lacking marker specificity and technical difficulties associated with mRNA, immunohistochemical (IHC) or flow cytometric (FACS) analysis of tissue-infiltrating immune cells could bring forth the above mentioned conflicting reports. Analysis of mRNA expression cannot be associated to cell numbers, since it determines an overall amount of a certain transcript. FACS is problematic for solid tissues, since dissociation into single cell suspension is required and IHC is semiquantitative.[28] Despite those issues the general view that anti-tumor response is directly associated with the activity of effector T-cells and its balance with Treg is unchallenged.

Cytosine methylation of CpG dinucleotides covalently alters DNA.[29] It is directly associated with inaccessible chromatin, whereat demethylation determines DNA-accessibility to the transcriptional machinery. Regulation via differential methylation contributes to transcriptional control.[30] During bisulfite-conversion of genomic DNA, unmethylated CpGs are converted to TpG ("TpG-variant"), whereas methylated CpGs remain as CpG residues ("CpG-variant")[31] allowing the discrimination between both variants. Exploitation of epigenetic mechanisms as tool for cell quantification was suggested[32,33] and "epigenetic immunophenotying" based on measurement of bisulfite-converted FOXP3 TSDR to identify and distinguish Treg (as TpG variant) from all other cell types, including activated, FOXP3-expressing effector T-cells (as CpG variant) in mice and humans was established.[34] FOXP3 TSDR was confirmed as Treg marker of unequalled specificity.[35] Advantageously, this assay format uses DNA as analyte, a stable substrate with predetermined copy numbers per cell. No detection thresholds arbitrarily segregate positive from negative cells, and this analysis can be performed on cell suspensions, solid tissues or body fluids with no particular demands on conservation states.

In analogy to FOXP3-TSDR, here we determined the epigenetic pattern of the intergenic CD3G/CD3D region as specific marker for identification of oTL. We developed a highly sensitive qPCR and provided an epigenetic reference system for total cell number determination. Applying these epigenetic assays, we analyzed tissue-infiltrating Treg and oTL in bronchial, colorectal and ovarian (tumor) tissues. Our data show that oTL-infiltration in tumors correlates with patient prognosis and the Treg-to-oTL ratio is significantly dysbalanced in tumors.

Results

Cell type specific gene regions susceptible for complete bisulfite-conversion. We tested bisulfite-convertibility of CpG-dinucleotides in the intergenic region of CD3D/CD3G and the CpG-island in GAPDH by means of bisulfite-sequencing (**Fig. 1**). We found that all CpGs of the CD3 region were completely converted to TpGs in $CD4^+$ (including Treg) and $CD8^+$ T-lymphocytes. Bisulfite-conversion in granulocytes, monocytes, B-lymphocytes and NK-cells resulted in the CpG-variant only. We exclusively found the TpG-variant in GAPDH in all tested immune cell types and confirmed this in various tissues (data not shown). Next, we designed quantitative real-time PCR assays (qPCR) for CD3 and GAPDH. For each region, we developed one qPCR system that exclusively recognizes the TpG-template, and one that is specific for the CpG-template (**Fig. 1C**). In order to provide a copy number quantification standard, we constructed plasmid systems for both loci that correspond to TpG- and CpG-variants. We showed linearity of amplification over three orders of magnitude (amplification efficiency: 1.95–2). We did not detect cross-reactivity of each TpG- and CpG-variant specific qPCR with the mutually opposite template.

Characterization of epigenetic qPCR assays. CD3 and GAPDH qPCRs were analyzed on separated blood cell fractions purified according to Baron et al.[34] Using serial dilutions of plasmids containing the equivalent of bisulfite-converted TpG or CpG DNA target regions as standard, we determined DNA copy numbers. The ratio of TpG/(TpG + CpG) copies was calculated for each gene region. The results indicate that $CD8^+$ and $CD4^+$ T-cells contain above 99% TpG-variant for the CD3 locus, while $CD19^+$ B-cells, $CD15^+$ granulocytes, $CD14^+$ monocytes, $CD3^-CD56^+$ NK-cells consist exclusively (>99%) of the CpG-variant. Targeting the GAPDH locus showed that amplification of the CpG-variant failed, whereas the TpG-variant was amplified efficiently in all cell types. Hence, quantitative analysis of GAPDH demethylation provides a cell type independent marker to detect total DNA copy number of all cells in a given sample. Furthermore, the specificity of the CD3, FOXP3 and GAPDH qPCR assays were tested on tumor cell lines originating from bronchial, colorectal and ovarian cancers. All tumor cell lines were found exclusively as CpG variants in both CD3 and FOXP3 loci. In the GAPDH locus all three cell lines were only detected in the TpG variant (**Table 1**).

To further demonstrate technical accuracy of the qPCR assays, we performed DNA spiking experiments. For this, we selected FACS purified regulatory T-cells, whose bisulfite-converted DNA consist of >99.5% of the TpG-variant and granulocyte DNA, which consist to >99.7% of the CpG-variant in both, CD3 and FOXP3 loci. Using plasmids containing sequences identical to the TpG- and CpG-variants of the regions in CD3, FOXP3 TSDR, and the TpG-variant of GAPDH for normalization, we quantified the relative amount of CD3 and FOXP3 TpG-variants compared to the overall cell number. For this, we artificially spiked 40, 20, 10, 5, 3, 2 and 1% Treg DNA into a background of granulocyte DNA. Using the GAPDH and the cell-type specific TpG-variants of the DNA systems for relative

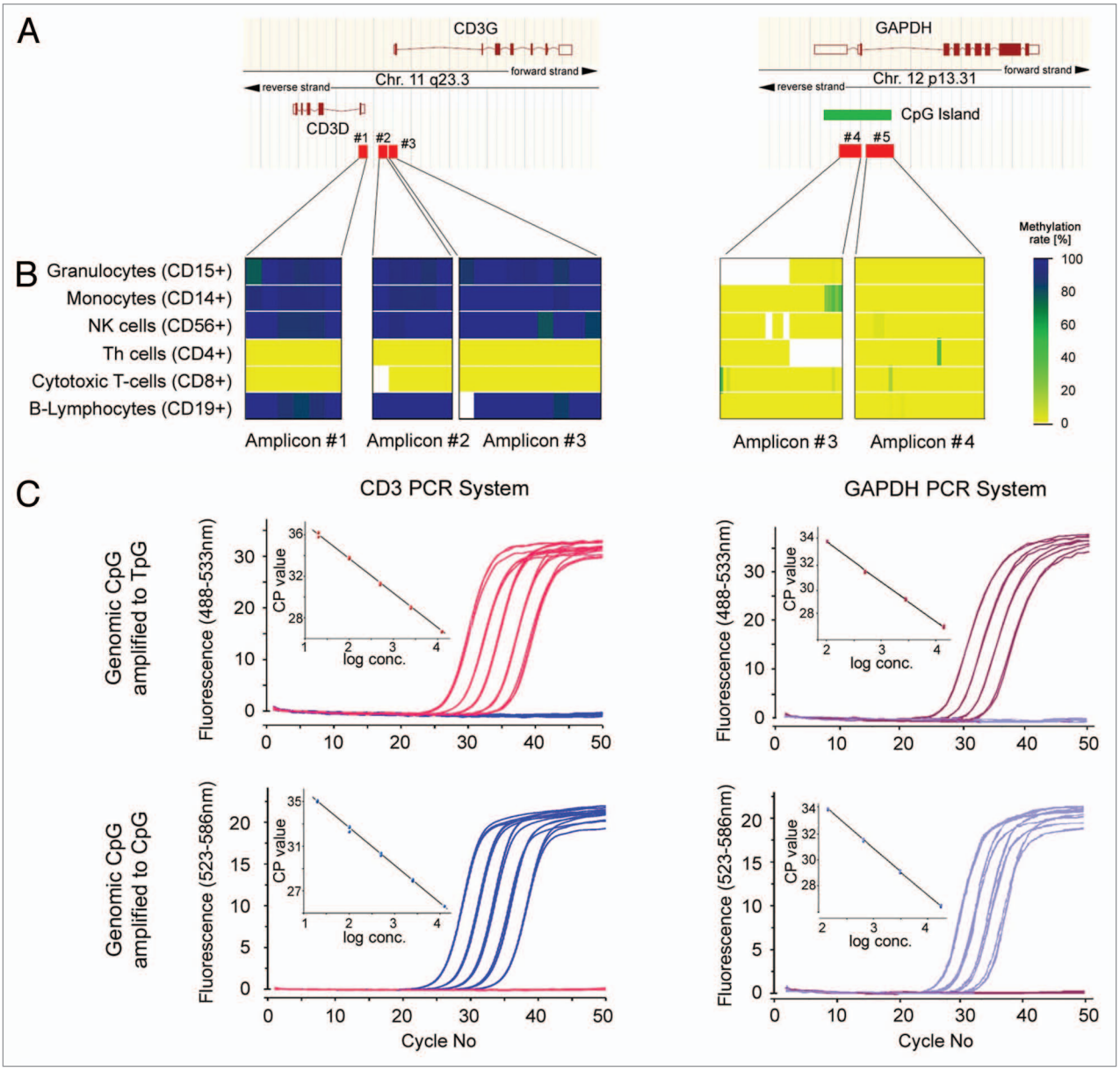

Figure 1. Epigenetic profiling of the CD3 and GAPDH loci. (A) Genomic localization and organization of the genes. Transcripts are shown depending on their orientation above or below the chromosomal bar. Amplicons used for epigenetic analysis are indicated as red boxes. (B) Epigenetic profiling obtained from bisulfite-sequencing of amplicons shown in (A). Each line represents the bisulfite-conversion status of CpGs in the amplicon tested on purified cell types indicated left. Individual squares represent single CpG-positions. Blue squares correspond to the CpG-variant and yellow squares to the TpG-variant. The color code is shown on the right hand side. (C) Amplification profiles of bisulfite-conversion specific qPCRs. Upper parts: qPCR specific for TpG-variant tested on dilutions of 12,500, 2,500, 500, 100 and 20 plasmid copies representing TpG (red) and CpG template variants (blue). Lower parts: The same experiment using qPCR specific for the CpG-variant. Linearity of qPCRs is shown inside each graph by plotting CP-values over log-concentration of template.

quantification, we found strict correlation between the theoretically assumed values for the spiked samples and CD3 and FOXP3 qPCR measurements (**Table 2**).

Analysis of Treg and overall T-lymphocytes in whole blood samples. The epigenetic markers for Treg and overall T-lymphocytes (oTL) were tested on 17 whole blood samples. Results were compared with data obtained by FACS analysis on the same samples using the lineage specific surface molecules CD4 and CD25 for Treg and CD3 for oTL. The proportion of $CD3^+$ cells as determined by FACS strictly correlates to the proportion of the TpG-variant as determined by CD3 qPCR (Spearman-R = 0.78; p = 2.0E-4) (**Fig. 2A**). Similarly, comparison of the proportion of $CD4^+CD25^+CD127^-$ cells obtained by FACS with TpG DNA found for the FOXP3 TSDR locus showed a strong correlation (Spearman-R = 0.74, p = 7.0E-4). The FOXP3-to-CD3 ratios, i.e., the ratios of Treg to oTL, measured by either FACS or qPCR were also strongly correlated (Spearman-R = 0.7, p = 1.8E-3). For comparison, Spearman rank correlation was used since

Table 1. Validation of qPCR assays on isolated blood cell fractions

Immune cell type/tumor cell line		FOXP3 assay			CD3 assay			GAPDH assay		
		Copy number		Ratio [%]	Copy number		Ratio [%]	Copy number		Ratio [%]
		TpG	CpG	TpG/(TpG + CpG)	TpG	CpG	TpG/(TpG + CpG)	TpG	CpG	TpG/(TpG + CpG)
Granulocytes	$CD15^+$	For data, see ref. 40			4.3	1513.8	0.28	2060.5	0.46	99.98
Monocytes	$CD14^+$				0	873.0	0	1154.3	0	100
NK cells	$CD56^+$ $CD16^+$ $CD3^-$				2.3	218.8	1.02	317.5	0	100
NK T-cells	$CD56^+$ $CD8^-$ $CD3^+$				n.d.	n.d.	n.d.	232.1	0	100
Th cells	$CD4^+$				1009.4	1.6	99.84	772.7	0	100
Regulatory T-cells	$CD4^+$ $CD25^+$ $FOXP3^+$				2726.2	3.6	99.87	2197.4	0	100
Memory cytotoxic T-lymphocytes	$CD8^+$ $CD45RA^-$ $CCR7^-$				488.6	0.8	99.83	384.5	0	100
Naive cytotoxic T-lymphocytes	$CD8^+$ $CD45RA^+$ $CCR7^+$				1859.9	4.3	99.77	1475.1	0.41	99.97
B-lymphocytes	$CD19^+$				0.6	161.9	0.38	224.1	0	100
Lung carcinoma cell line A549		12.7	1653.6	0.76	6.2	587.3	1.05	1740	0	100
Ovarian carcinoma cell line SCOV6		8.5	1045.5	0.81	4.6	1313.3	0.35	9582.9	0	100
Colorectal carcinoma cell line HCT116		0.0	829.2	0.0	2.6	885.7	0.29	8025.3	0	100

Table 2. Technical accuracy of qPCR assays

	Calculated ratio [%]			
	FOXP3 assay		CD3 assay	
Target cells spiked in [%]	TpG/(TpG + CpG)	TpG/TpG^{GAPDH}	TpG/(TpG + CpG)	TpG/TpG^{GAPDH}
0.0	0.0	0.0	0.6	0.9
1.0	1.0	1.4	1.4	1.7
2.0	1.7	2.5	2.5	3.0
3.0	2.6	3.9	3.6	4.5
5.0	4.3	6.1	5.9	6.9
10.0	8.7	12.2	11.4	13.4
20.0	20.5	25.8	22.1	26.5
40.0	37.2	46.5	42.4	47.8
Pearson correl. coeff. [rho]	1.0	1.0	1.0	1.0

goodness-of-fit testing according to Kolomov-Smirnov revealed significant deviations from normal distributions for FACS, indicating a high number of outliers, while accepting normal distribution for qPCR. Since Treg are a subgroup of oTLs, we investigated interdependence of these two populations (**Fig. 3**). We observed that—in whole blood—the oTL and Treg frequencies correlate with each other with noticeable Spearman correlation (R = 0.47, p = 3.8E-8).

qPCR analysis of FOXP3 TSDR and CD3 in solid healthy and tumor tissues. To provide a quantitative evaluation of tissue-infiltrating $FOXP3^+$ regulatory T-cells (Treg) and overall $CD3^+$ T-lymphocytes (oTL) in solid tissues, we compared DNA isolated from healthy and tumorous tissue of ovarian, bronchial and colorectal origin (**Fig. 4A–C**). The median frequency of infiltrating immune cells in healthy ovarian tissue (OT) is at 0.12% and 4.27% for Treg and oTL, respectively. For pathologically confirmed ovarian cancer samples (OvCa), we observed a median of 1.28% Treg and 7.76% oTL. According to the non-parametric Wilcoxon rank sum test for independent samples, elevation of both parameters in tumors compared to healthy tissue is statistically highly significant (p_{Treg} = 2.34E-11; p_{oTL} = 0.0066; **Fig. 4A and B**). In healthy bronchial tissue (BT) 2.0% Treg and 29.6% oTL were observed. When testing adjacent tumor lesions (BCa), we observed 4.2% Treg and 22.3% oTL. Both higher Treg and lower oTL frequencies in tumor compared to healthy tissue are statistically significant according to the Wilcoxon signed rank test (p = 0.0024 and p = 0.0015; **Fig. 4A and B**). The same analysis was conducted with two independent colorectal cancer cohorts comparing healthy, tumor-adjacent (CT) with tumor tissue (CRC). In the first cohort, we observed median Treg and oTL frequencies of 1.9% and 33.5% in healthy (CT-I), respectively and 3.8% Treg and 26.1% oTL in tumor (CRC-I) tissue, respectively (**Fig. 4A and B**). Wilcoxon signed rank test indicates that higher Treg proportions (p = 3.80E-4; **Fig. 4A**) and reduced oTL proportions (p = 1.0E-4; **Fig. 4B**) in the tumor is statistically significant. All statistical analyses remain significant after correction for multiple testing. Data from CRC-II cohort confirmed this observation showing 1.8% Treg and 32.3% of CD3 cells in healthy (CT-II), contrasted by 4.3% Treg and 23.9% oTL in tumor (CRC-II) samples (p = 1.0E-4 and p = 0.0296) for Treg and oTL, respectively). When correcting for multiple testing the differences between healthy and tumorous Treg and oTLs in the CRC-II cohort, oTL-values drop below statistical significance (p = 0.1), but the relevance of the trend remains undisputed.

For all four cohorts, we analyzed the ratio of Treg-to-oTL (**Fig. 4C**). In healthy tissues, the median relative Treg level within the oTL ranged between 3–8% ($median_{OT}$: 3.4%, $median_{BT}$: 7.6%, $median_{CT-I}$: 5.9%, $median_{CT-II}$: 7.8%). In tumor entities,

this ratio is shifted towards an increased proportion of Treg (median$_{OvCa}$:19.7%, median$_{BCa}$:18.3%, median$_{CRC-I}$:17.5%, median$_{CRC-II}$:21.6%). All changes are statistically highly significant ($p_{OvCavs.OT}$ = 8.06E-07, $p_{BCavs.BT}$ = 1.59E-14, $p_{CRC-Ivs.CT}$ 3.05E-13, $p_{CRC-IIvs.CT-II}$ p = 5.10E-7). Since for bronchial and colorectal patient cohorts donor-matched pairs of tumor and adjacent healthy tissue were used, we directly compared Treg-to-oTL ratios in donor-matched analysis, excluding effects from donor-to-donor variations. We found that 93.5% (43 out of 46) of pairs show an increase of the Treg-to-oTL ratio in bronchial tumor (BCa) compared to healthy adjacent tissue (BT). In the CRC-I cohort we found an equivalent increase in 81% (39 of 48) of cases and in CRC-II cohort this increase is observed in 86% (71 of 83) of pairs.

We also investigated the interdependence of Treg and oTL (**Fig. 3**). Similar to the correlation found in whole blood samples, we observed a noticeable correlation between Treg- and oTL-infiltration in healthy bronchial tissue (Spearman-R = 0.68, p = 8.6E-08) and colon tissue (R_{CT-I} = 0.55, p = 4.4E-5, R_{CT-II} = 0.54, p = 2.1E-8). The same analysis with a limited number of ovarian tissue samples (N = 13) did not show significant correlation (R = 0.15, p = 0.6). When testing this interdependence in diseased tissues we observed strong correlation in ovarian cancer tissue (R_{OvCa} = 0.77, p = 3.5E-21), and noticeable correlation in BCa and CRC (R_{BCa} = 0.48, p = 3.25E-8; R_{CRC-I} = 0.37, p = 0.02; R_{CRC-II} = 0.58, p = 1.2E-10).

Correlating patient survival with intratumoral immune cell levels. For colorectal and ovarian cancer patients, follow-up data were available. Hence, we tested if the frequency of tumor-infiltrating oTLs correlated with patient prognosis (**Fig. 5**). To detect the effect exhibited by the oTL frequencies, we split patients at the median oTL frequency into two groups. This split is arbitrary, but provides for balanced sampling sizes. In CRC cohort-I, 20 recurrences—reporting the endpoint of progression-free survival (PFS)—and 10 deaths, endpoint of the overall survival (OS), were reported with 77 and 90 censored data points, respectively. These event numbers were not sufficient for statistically significant survival analyses, but a trend for an improved PFS and OS was observed for patients with high frequencies of oTL. Less than 10% of the patients with high and approx. 25% of patients with low oTL frequencies had suffered recurrence after 20 months. 5% of patients with high and 15% of those with low levels of oTL had died 40 months after diagnosis (**Fig. 5**). We then used an independent colorectal cancer cohort (CRC-II) excluding stage I disease patients to confirm the observed trend. In this cohort, 80 patients had sufficient follow-up with 39 recurrences and 30 deaths reported. The median oTL frequency in this cohort was at 23.9% (range: 4.9–72.1%). In univariate Kaplan-Maier analysis for PFS we found a clear trend towards better survival of patients with high oTL frequencies (median 82 vs. 40 months). Median OS was not reached for patients with high oTL, and was at 80 months for low oTL frequencies indicating a statistically significant survival advantage (p = 0.039). In this cohort, we also determined the oTL numbers using IHC. Those data did not correlate with a better prognosis or with data found in the epigenetic analysis (**Fig. 6**). In the OvCa cohort, data from 67 patients were included in the PFS-analysis with 45 recurrences reported.

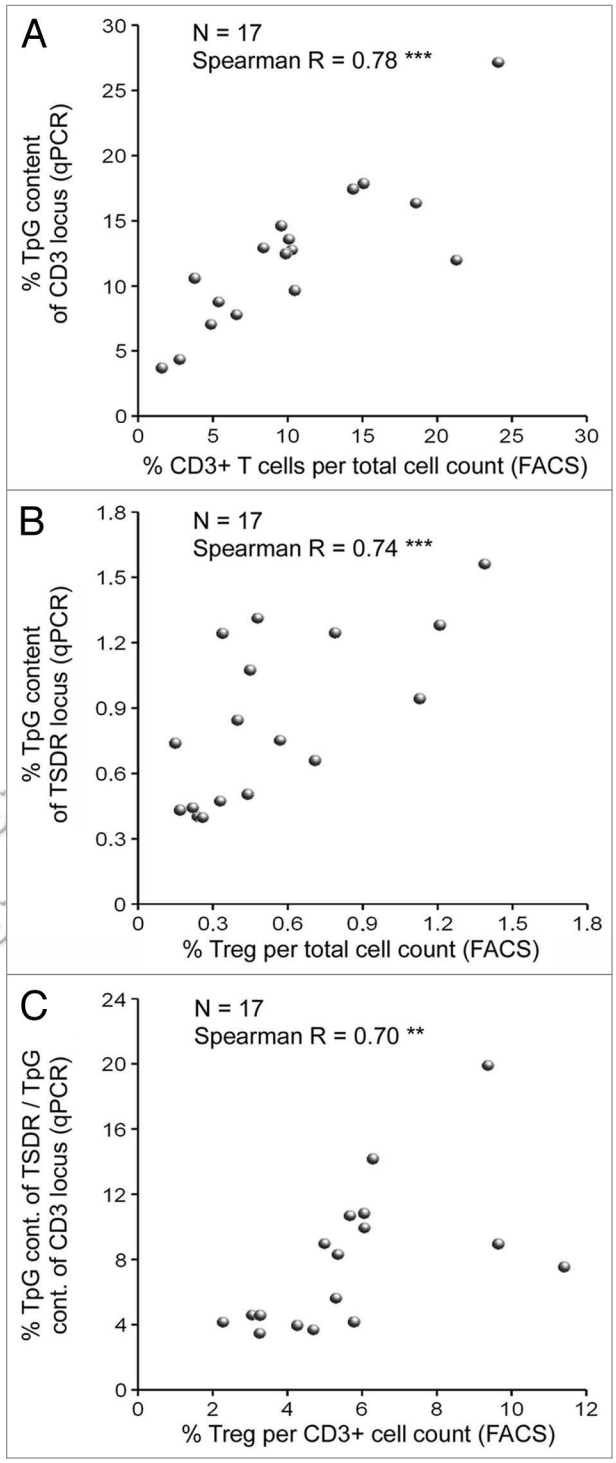

Figure 2. CD3$^+$ and FOXP3$^+$ cell counting using epigenetic qPCR and FACS. Peripheral blood was collected from 17 donors. Cell frequency was determined by FACS (X-axis) and qPCR analysis (Y-axis). (A) Cell frequencies determined by FACS describe the percentage of CD3$^+$ cells per all nucleated cells. qPCRs were performed applying the CD3-specific qPCR system. (B) Cell frequencies determined by FACS describe the percentage of CD4$^+$CD25$^+$CD127$^-$ cells. qPCRs were performed using the FOXP3-specific qPCR system. (C) Cell frequencies determined by FACS describe the percentage of CD4$^+$CD25$^+$CD127$^-$ cells within CD3$^+$ cells. R indicates Spearman rank correlation coefficient for FACS compared to qPCR measurement. Statistical significance is indicated as follows: **p ≤ 0.01; ***p ≤ 0.001.

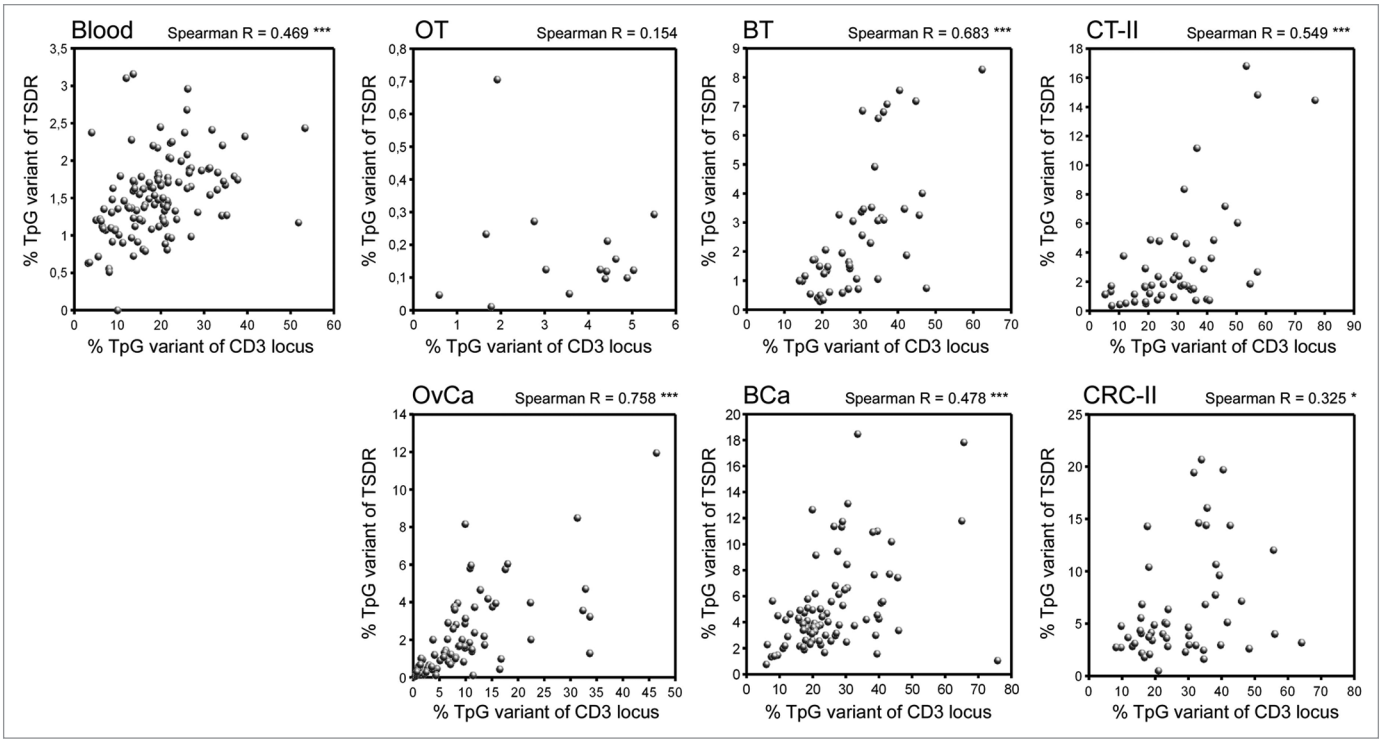

Figure 3. Correlation of CD3⁺ T-cells with Treg in various tissues. CD3⁺ T cell levels (X-axis) are plotted against Treg levels (Y-axis). Cell frequencies were derived from measurements of the TpG variants in the CD3 intergenic region and the FOXP3 TSDR. Analysis was performed for whole blood, ovarian (OT), lung (BT) and colorectal tissue (CT-II) as well as for ovarian (OvCa), bronchial (BCa) and colorectal (CRC-II) cancer. Correlation between the two parameters is indicated by the Spearman rank correlation coefficient Rho, and the p-value is given as parameter for significance. Each dot indicates a single sample measured with both the CD3 and FOXP3 qPCR assay.

For OS analysis, 79 patients were included and 30 events were reported. Univariate analysis in the OvCa cohort suggests better prognosis for patients with oTL frequencies higher than the median of 7.76% (**Fig. 5**). Median PFS was 40 months for patients with high and 25 months with low levels of oTL. Similarly, median OS was better for patients with high oTL (70 months) compared with patients with low oTL frequencies (52 months).

For PFS and OS of all three cohorts, we calculated Cox regression models. The effect of continuously increasing oTL is protective throughout all analyses, also after adjusting for age, grading, stage and other cohort-specific parameters (**Table 3**). The hazard ratio for PFS is at 0.966 and 0.998 for OvCa and CRC-II, respectively and at 0.98 and 0.987 for OvCa and CRC-II for OS. For CRC-I, the small number of events disallows robust modeling, but—with tentative hazard ratios of 0.995 and 0.972 for PFS and OS, respectively—the trend for improved tumor response mediated by elevated T-lymphocyte levels is further confirmed. Together, Cox regression analysis shows that risk for recurrence or death decreases by approx. 0.2–3.4% for each 1% increasing oTL-content in the tumor environment.

Discussion

Our data demonstrate that the intragenic CD3G/CD3D region is accessible for bisulfite-conversion in CD3⁺ T-cells only. Based on this characteristic property a specific qPCR assay for sensitive quantification of T-lymphocytes was designed. Together with the FOXP3 qPCR assay,[40] these assays present a suitable technical approach for quantification of oTL and Treg. A region within the CpG-island of the housekeeping gene GAPDH—which is bisulfite-accessible in all cell types—can be used to determining total cell numbers. Cloning the corresponding target regions of FOXP3, CD3 and GAPDH on a single plasmid as equimolar quantification standard, allows for comparable analysis of named cell types. Since measurements are performed on frozen or paraffin-embedded samples and results correlate with cell counts obtained from FACS with fresh samples, this technology lends itself to application in clinical trials and routine diagnostics, where sample management remains a core challenge.

Here, the technology was applied to elucidate the role of immune cells in tissues of patients with solid ovarian, bronchial and colorectal tumors. Our data show significantly lower infiltrates of Treg and oTL in healthy ovarian tissues compared to other analyzed tissues. Nonetheless, the mean ratio of Treg-to-oTL stably ranges between 3.5–7% in all healthy tissues, which corresponds to the ratio measured in peripheral blood and was reported elsewhere using FACS analysis.[17,18] This suggests that healthy immunological balance is obtained when up to one tenth of T-lymphocytes exhibit a suppressive phenotype. In all tested tumor entities, we observed higher Treg frequencies. oTL levels were reduced in lung and colorectal but increased in ovarian tumor samples. Given that T-lymphocyte frequencies were

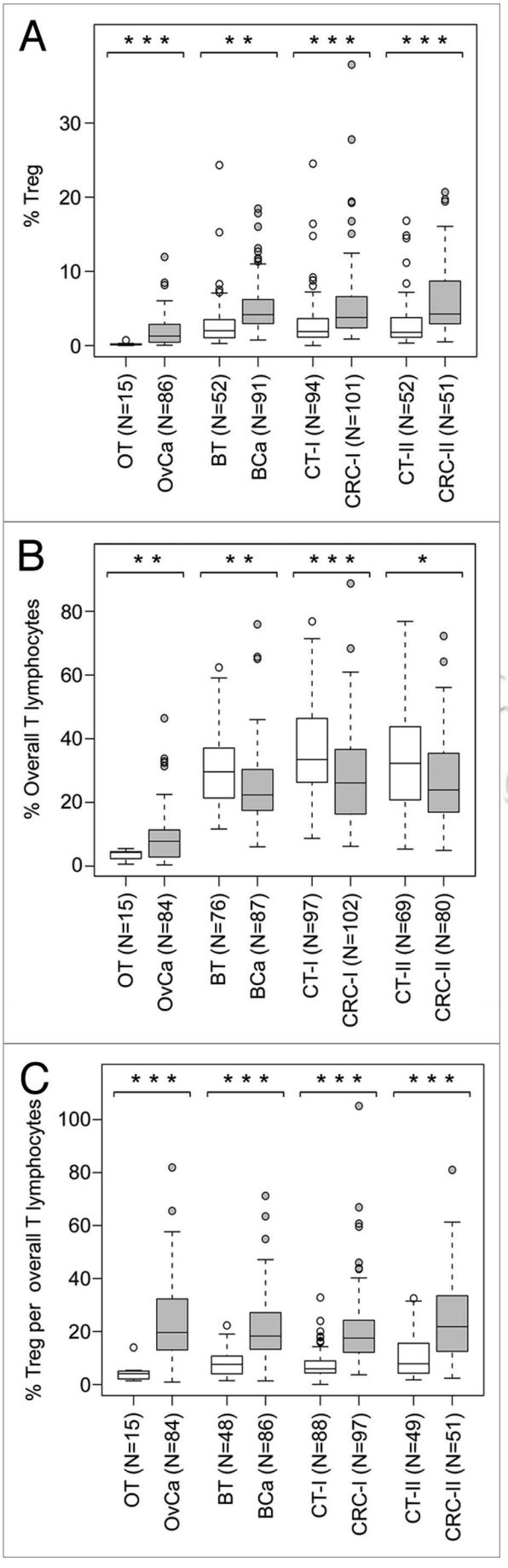

Figure 4. Frequency of tissue-infiltrating lymphocytes. Boxplots showing percentages of (A) Treg, (B) $CD3^+$ T-cells, (C) Treg within $CD3^+$ T-cells in healthy and cancerous tissues. N indicates the number of patients included in each plot. The box depicts the middle 50% of the distribution. The line in the box represents the median. Whiskers extend to include 95% of all data. Outliers are indicated by circles. The statistical significance is indicated as follows: *p ≤ 0.05, **p ≤ 0.01, ***p ≤ 0.001.

lower in healthy ovarian tissue than in other tissues, we assume that enhanced Treg- and oTL-level are owed to tumor-mediated increase of stroma density and vascularization. The ratio of Treg-to-oTL was determined to access the immune status excluding density and vascularization-associated factors. We observed at least a doubling of median Treg-levels within all tissue-infiltrating T-cells in tumors. Notably, this shift was observed throughout all tumor entities and cohorts. Furthermore, our matched-pair analysis showed relative enrichment of Treg in 153 out of 177 (86%) patients. Exceptions to this trend were mainly observed in colorectal samples. Since histological tissue allocation is particular demanding in those samples, we consider technical problems at tissue selection a feasible explanation for outliers.

Our data blend in with many reports suggesting that tumor control is achieved through Treg-depletion[21] and increased frequency of effector T-cells.[7,8] $CD25^+FOXP3^+$ cells show upregulation in tumor tissues.[17] Low levels of $CD25^+CD4^+FOXP3^+$ cells[9] and high levels of CD3 mRNA[11] have been associated with better survival of cancer patients. Jointly those data pointed strongly towards a role of Treg and T-lymphocytes in tumor establishment. However, human studies were afflicted with the problem that $CD25^+FOXP3^+$ cells include activated effector T-cells and tissue analysis using either mRNA, IHC or FACS analysis only provides limited accuracy of quantification. Using a different technical approach, here we showed that a dysbalance of Treg-to-oTL infiltrates is a prominent observation in solid tumors. The uniform dysbalance throughout various tumor entities suggest that this effect is a consistent defect of the tumor-associated immune status. We hypothesize that this dysbalance contributes to the body's pathological inability to counteract tumors, and may be prerequisite for permanent tumor establishment.[19]

We also tested the role of T-lymphocyte infiltration in tumors on patient survival. Our data corroborate previous reports, which indicate that increased frequencies of intratumoral oTL lead to better prognosis.[10,11] This trend is observed for all three independent studies for progression-free survival (PFS) and the associated overall survival (OS) analyses. Although for the individual cohorts statistical significance is not reached, qualitative equivalence of a strong trend throughout all cohorts for both PFS and OS indicate high relevance of this observation. In the current analysis, epigenetic analysis surpasses the prognostic capability of IHC measurements, since high oTL counts in IHC did not correlate with better prognosis. Previous reports using larger cohorts, however, confirm the prognostic value of oTL when applying IHC.[41,42] This fact might be interpreted in two ways; on one hand it is possible that the robustness and/or sensitivity of IHC measurements are restricted and larger cohorts are generally required in order to achieve the prognostic information. Alternatively, we used TMAs and were not able to analyze either the entire tumor

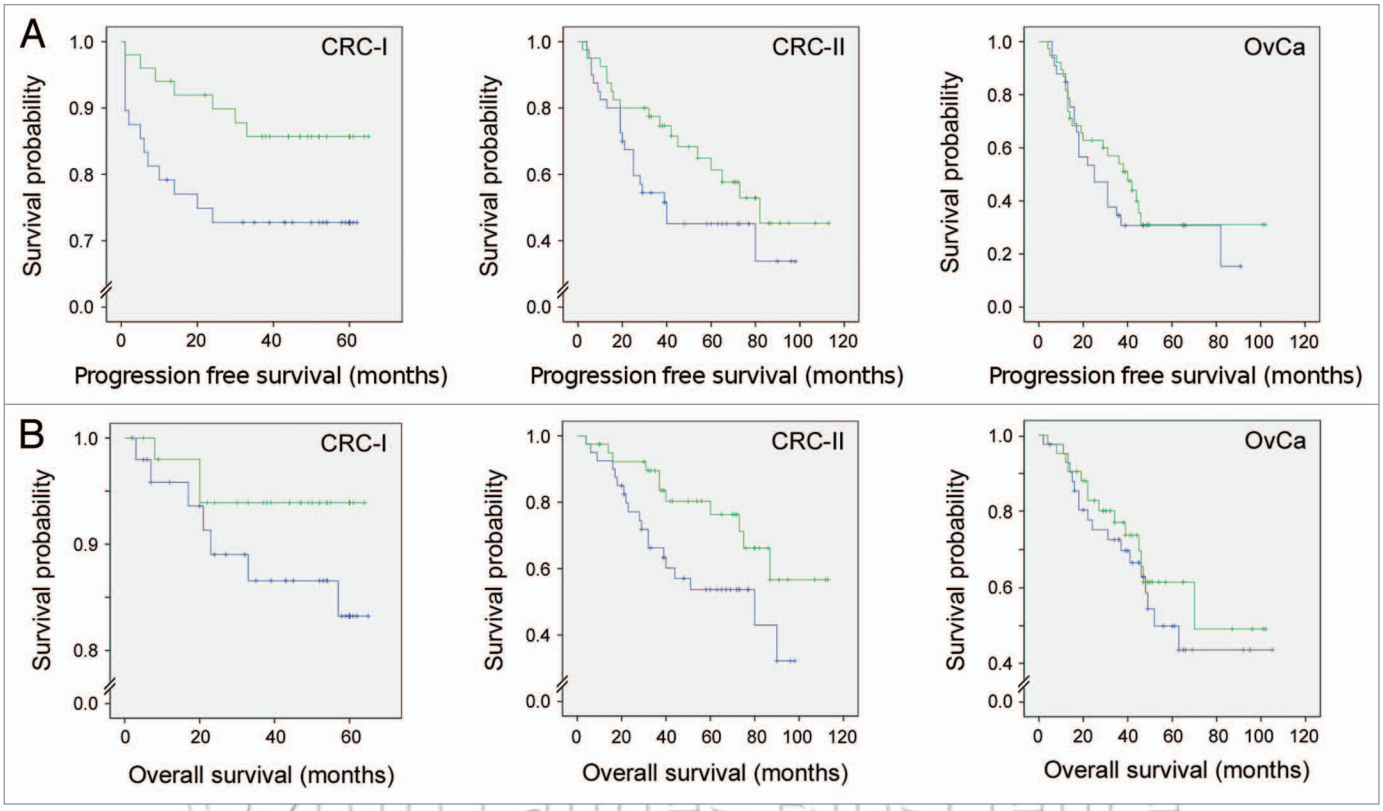

Figure 5. Cumulative survival of colorectal and ovarian cancer patients. Samples from each tumor entity were devided into two groups at their median value of tumor-infiltrating overall T-lymphocytes (oTL) as measured by CD3-specific qPCR. Levels above median (high oTL frequencies), green; levels below median (low oTL frequencies), blue. (A) Progression free survival (PFS). In the left (CRC-I; median = 26.1%; $N_{high} = 7$; $N_{low} = 12$) and middle (CRC-II; median = 23.9%; $N_{high} = 17$; $N_{low} = 22$) part colorectal cancer samples are shown. The right part shows ovarian cancer samples (OvCa; median = 7.76%; $N_{high} = 23$; $N_{low} = 23$). (B) Overall survival (OS). Left part: CRC-I cohort ($N_{high} = 3$; $N_{low} = 7$); middle part: CRC-II cohort ($N_{high} = 11$; $N_{low} = 19$); Right part: OvCa cohort ($N_{high} = 14$; $N_{low} = 18$).

or to select highly specific areas, such as the invasive margin for analysis leading to the failure to detect the prognostic value. Either way, these data give room for the thought that the development of an epigenetic measurement system of tissue-infiltrating $CD3^+$ cells may proof a less investigator-dependent and hence better standardizable routine tool for its use as prognostic marker. However, before such aim can be addressed, larger cohort studies will be required to unequivocally manifest prognostic values of the epigenetic system for all analyzed tumor entities.

The positive effect of oTL is in line with the hypothesis that tumor-infiltrating T-lymphocytes directly influence evolving tumors. On the other hand, our data show the difficulty for the interpretation of prognostic data that comes from the interdependence of Treg and oTL levels. In all tissues, Treg abundance is heavily influenced by oTL levels and, possibly as a consequence, an inverse correlation between Treg-to-oTL levels and survival is not observed (**Suppl. Fig. 1**). Hence, the assumption that increased overall Treg frequencies leads to worse prognoses appears over simplistic. Our attempts to calculate Cox regression models using oTL levels as covariate for Treg-to-oTL frequencies were aimed at ameliorating this problem, but resulted in inconclusive data due to limited cohort sizes. Hence, from the current study we are incapable of showing consistent effects of the Treg-to-oTL ratios on patient survival. To investigate the effect of Treg-to-oTL including T-lymphocyte levels as a covariate and other confounding errors will require the analysis of larger cohorts.

In summary, we present evidence that epigenetic analysis of immune cells is a novel method that facilitates immunophenotyping in blood and, possibly more importantly, in solid tissues. The shown data firmly establish a prominent role of the ratio of Treg-to-oTL during tumor establishment. Despite lack of formal prove, our data doubtlessly promote the view that dysbalance between suppressive Treg and effector T-lymphocytes may be an intrinsic characteristic of tumor establishment. Hence, altering the ratio of tolerogenic-to-effector immune cells may be a strong target for anti-tumor strategies. The positive effect of increasing intratumoral T-lymphocyte frequencies on the prognosis of patients further supports the view that the balance of immune cells is an important part of the bodies failing anti-tumor response.

Materials and Methods

Tissues and cell lines. FFPE samples were retrieved from the archives of the Institute of Pathology, Charité, Campus Benjamin Franklin. Fresh ovarian tissue and blood was retrieved

from tumor bank ovarian cancer, Charité, Campus Virchow. Tumor cell lines A549 (lung), SCOV6 (ovarian) and HCT116 (colorectal) were obtained from U. Ziebold, Max-Delbrück-Center for Molecular Medicine, Berlin.

Isolation and bisulfite-conversion of genomic DNA. DNA was purified using DNeasy Blood&Tissue Kits (Qiagen). DNA from FFPE samples was isolated using QIAampDNA FFPE TissueKit (Qiagen). Tissue section thickness was adjusted to 10 μm. Reactions were carried out using 10 tissue sections. Bisulfite-conversion was performed using EpiTect BisulfiteKit (Qiagen) using 0.5–1 μg genomic DNA.

Oligonucleotides. Oligonucleotides (forward (fp), reverse (rp) primers and probes (p)) are indicated by chromosomal positions of human genome assembly GRCh37 (e!Ensemble release56; Sep.09).

Bisulfite-sequencing. (a) intergenic CD3G(ENSG00000160654)/CD3D(ENSG00000167286) region: Amplicon-No.1, fp:11:118213200-21:1, rp:11:118213616-37:1; No.2, fp:11:118214271-92:1, rp:11:118214685-705:1; No.3, fp:11:118214702-23:1, rp:11:118215151-73:1; (b)GAPDH(ENSG00000111640): No.3, fp:12:6644119-35:1, rp:12:6644635-56:1; No.4, fp:12:6643586-604:1, rp:12:6643990-4011:1.

RT-PCR. (a) FOXP3(ENSG00000049768): CpG-specific: fp:X:49117219-46:1, rp:X:49117283-307:1, p:X:49117256-73:1; TpG-specific: fp:X:49117219-46:1, rp:X:49117283-307:1, p:X:49117256-78:1. (b) CD3: CpG-specific: fp:11:118213633-53:1, rp:11:118213686-707:1, p:11:118213670-87:1; TpG-specific: fp:11:118213632-53:1, rp:11:118213686-709:1, p:11:118213664-90:1. (c) GAPDH: TpG-specific: fp:12:6644378-99:1, rp:12:6644456-76:1, p:12:6644429-57:1.

Bisulphite sequencing. PCR was performed in 25 μl containing 7 ng DNA, 1x PCR Buffer, 1 U Taq DNA polymerase (Qiagen), 200 uM dNTP, 12.5 pmol primer. Thermocycling conditions: 1 x 95°C, 15 min, 40x (95°C, 1 min; 55°C, 45s; 72°C, 1 min); 1 x 72°C, 10 min. PCR products were purified using ExoSAP-IT (USB Corp.,) and sequenced with amplification primers and BigDye Terminator v1.1 (Applied Biosystems). Products were Ethanol-precipitated, dissolved in 1 M betain and subjected to capillary electrophoresis on ABI 3100 genetic analyzer. AB1 files were interpreted using ESME.[36]

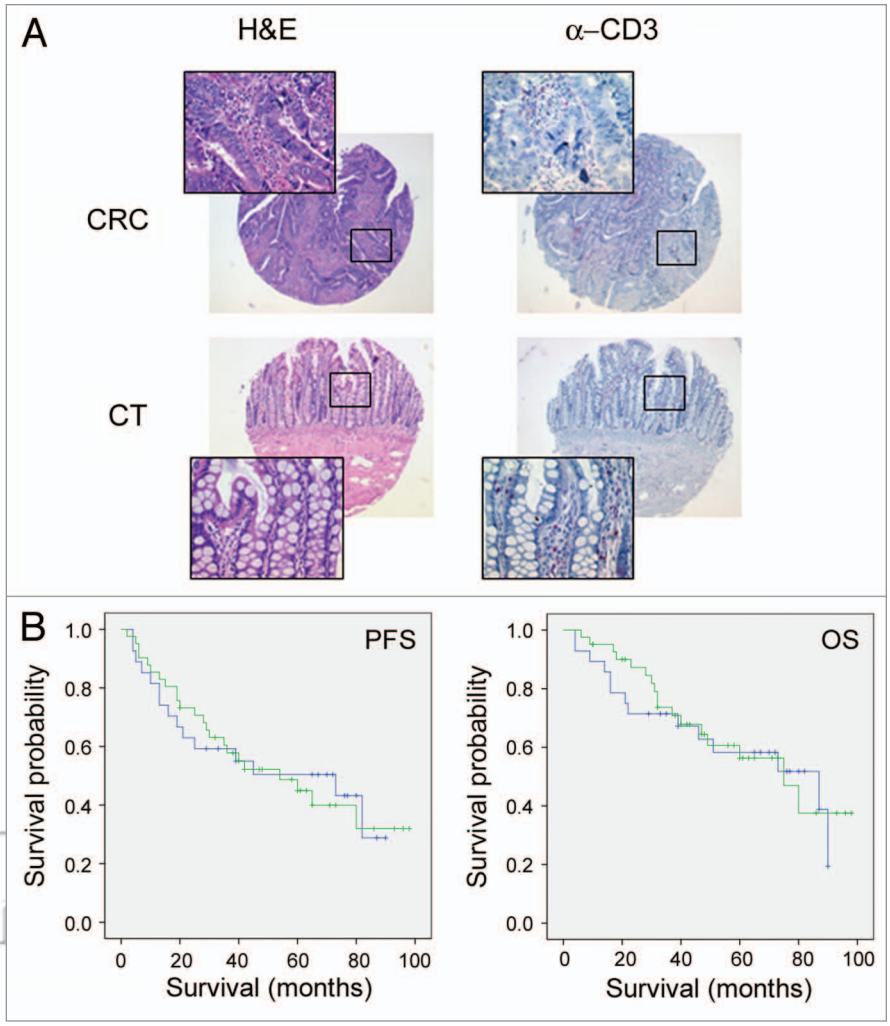

Figure 6. Quantification of tumor-infiltrating T-lymphocytes using immunohistochemistry. (A) illustrates a representative immuno-staining of colorectal cancer (CRC) and normal colonic mucosa (colon tissue; CT) sections prepared from tissue micro arrays. Overall T-lymphocytes (oTL; red, membranous) and regulatory T cells (Treg; red, nuclear) were stained using antibodies directed against CD3 and FOXP3, respectively. H&E represents hematoxylin/eosin staining. Original magnification: x20; inset: x80. (B) Kaplan-Meier plots illustrating cumulative survival of patients with colorectal cancer. Both, oTL and Treg were counted in cores of 1 mm in diameter and were used to perform PFS and OS analysis. Tumor samples were divided into two groups at their median level of oTL (median = 195). Levels above the median ("high") are represented by a green line and levels below the median ("low") are represented by a blue line. Sample numbers are as follows: oTL: N_{high} = 23, N_{low} = 15 for PFS; N_{high} = 17, N_{low} = 14 for OS. Treg: N_{high} = 19,N_{low} = 18 for PFS; N_{high} = 16,N_{low} = 15 for OS.

qPCR. qPCR was performed using Roche LightCycler 480 chemistry or Epitect-MSP (Qiagen) in 20 μl containing 30 pmol of each primer, 5 pmol probe, 50 ng λ-phage DNA and 60 ng DNA-template or corresponding amounts of plasmid. Samples were analyzed in triplicates. Cycling conditions were: 1 x 95°C, 10 min; 50x (95°C, 15s; 61°C, 1 min). Crossing points were computed by second-derivative method (LC480 software).

Plasmid standard. Target regions for the various real-time PCR assays were designed in silico, synthesized (Genscript Inc.,) and inserted into plasmid pUC57. Plasmids were linearized and diluted in 10 ng/μl of λ-phage DNA (New England Biolabs)

Table 3. Cox regression model for ovarian and colorectal cancer cohorts

Ovarian Cancer (OvCa) Cohort								
	Progression Free Survival (PFS)				Overall Survival (OS)			
	Sample no. 67		Events 45	Censored 22	Sample no. 79		Events 30	Censored 49
Prognostic factor	beta	Stand. Err.	HR	p-value	beta	Stand. Err.	HR	p-value
T-cells	-0.035	0.018	0.966	0.055	-0.020	0.020	0.980	0.326
Age at diagnosis	-0.013	0.018	0.987	0.480	0.020	0.020	1.020	0.328
Grade 1	-14.483	854.572	0.000	0.987	-15.260	1574	0.000	0.992
Grade 2	-0.213	0.361	0.808	0.555	-0.370	0.445	0.690	0.406
Stage I	-1.772	0.806	0.170	0.028	-1.544	1.108	0.214	0.164
Stage II	NA	NA	NA	NA	-15.369	3060	0.000	0.996
Stage III	-0.354	0.420	0.702	0.399	-0.200	0.509	0.818	0.694
Colorectal Cancer (CRC) Cohort II								
	Progression Free Survival (PFS)				Overall Survival (OS)			
	Sample no. 80		Events 39	Censored 41	Sample no. 80		Events 30	Censored 50
Prognostic factor	beta	Stand. Err.	HR	p-value	beta	Stand. Err.	HR	p-value
T-cells	-0.002	0.015	0.998	0.871	-0.013	0.016	0.987	0.414
Sex (Male)	0.570	0.406	1.768	0.160	0.555	0.400	1.742	0.166
Age at diagnosis	0.019	0.024	1.020	0.416	0.051	0.023	1.053	0.026
Grade 2	-0.213	0.401	0.808	0.595	-0.309	0.411	0.734	0.452
Stage II	-0.273	0.452	0.761	0.546	-0.860	0.518	0.423	0.097
MLH1	1.280	0.563	3.594	0.023	1.247	0.603	3.481	0.039
MSH2	-14.409	1044	0.000	0.989	-14.238	1091	0.000	0.989
Chemo	-0.193	0.575	0.825	0.738	-0.030	0.568	0.970	0.958

Stage refers to UICC nomenclature in colorectal cancers and to FIGO stages in ovarian cancer. The highest categorial value for each categorial parameter was used as reference. References are: female, Grade 3, Stage 4, no MLH1, no MSH2 and no chemotherapeutic treatment.

to obtain qPCR standards with final concentrations of 12,500, 2,500, 500, 100 and 20 template copies per reaction.

Cell sorting. Peripheral blood samples were obtained from healthy donors according to local ethical committee approval. Fractionation into different leukocyte populations was performed as described previously.[34] Purities and viability of sorted cells was >97%.

Statistical analysis. Template copy numbers were estimated from calibration curves (using serial dilutions of plasmid-based standards) by linear regression on crossing points via second-derivative maximum method.[37] The mean was used to aggregate triplicate measurements. The proportion of gene-specific DNA was computed as ratio of specific TpG-variant and the sum of TpG- and CpG-variants or the number of GAPDH TpG-copies. Cumulative survival was calculated applying Kaplan-Meier analysis.[38] For univariate comparison, statistical significance was assessed using Cox-Mantel test.[39] For correlation, Spearman rank correlations were used. Median differences were tested with Wilcoxon rank sum (ovarian cohort) or Wilcoxon signed rank tests (bronchial and colorectal cohorts) depending on the sampling method. All p-values are two-sided. Statistics software SAS 9.2 (TS2M2) (SAS Institute Inc., Cary, USA) was employed.

Acknowledgements

Fresenius co-financed J.S. Technologiestiftung Berlin co-financed U.B., T.S., T.C., S.O. We thank Manfred Gossen and Ulrieke Ziebold for providing tumor cell lines. We are indebted to Michael Weber, Alexander Olek and Helge Riemer for their support.

Author Contribution

J.S., C.L., A.M., P.L. provided samples. C.L., P.L., T.C., U.H., I.T., T.S. performed experiments, and/or critically read manuscript, A.G. prepared cells, T.D. performed statistical analysis, M.K., J.G. provided follow-ups. U.B., S.O. designed study, performed experiments, interpreted results and wrote manuscript.

Note

Supplementary materials can be found at:
www.landesbioscience.com/supplement/Sehouli-EPI6-2-sup.pdf

References

1. Guiot C, Degiorgis PG, Delsanto PP, Gabriele P, Deisboeck TS. Does tumor growth follow a "universal law"? J Theor Biol 2003; 225:147-51.
2. Dunn GP, Bruce AT, Ikeda H, Old LJ, Schreiber RD. Cancer immunoediting: from immunosurveillance to tumor escape. Nat Immunol 2002; 3:991-8.
3. Dunn GP, Old LJ, Schreiber RD. The three Es of cancer immunoediting. Annu Rev Immunol 2004; 22:329-60.
4. Kung P, Goldstein G, Reinherz EL, Schlossman SF. Monoclonal antibodies defining distinctive human T cell surface antigens. Science 1979; 206:347-9.
5. Shankaran V, Ikeda H, Bruce AT, White JM, Swanson PE, Old LJ, et al. IFNgamma and lymphocytes prevent primary tumour development and shape tumour immunogenicity. Nature 2001; 410:1107-11.
6. Zhou G, Lu Z, McCadden JD, Levitsky HI, Marson AL. Reciprocal changes in tumor antigenicity and antigen-specific T cell function during tumor progression. J Exp Med 2004; 200:1581-92.
7. Baier PK, Wimmenauer S, Hirsch T, von Specht BU, von Kleist S, Keller H, et al. Analysis of the T cell receptor variability of tumor-infiltrating lymphocytes in colorectal carcinomas. Tumour Biol 1998; 19:205-12.
8. Diederichsen AC, Hjelmborg JB, Christensen PB, Zeuthen J, Fenger C. Prognostic value of the $CD4^+$/$CD8^+$ ratio of tumour infiltrating lymphocytes in colorectal cancer and HLA-DR expression on tumour cells. Cancer Immunol Immunother 2003; 52:423-8.
9. Sato E, Olson SH, Ahn J, Bundy B, Nishikawa H, Qian F, et al. Intraepithelial $CD8^+$ tumor-infiltrating lymphocytes and a high $CD8^+$/regulatory T cell ratio are associated with favorable prognosis in ovarian cancer. Proc Natl Acad Sci USA 2005; 02:18538-43.
10. Zhang L, Conejo-Garcia JR, Katsaros D, Gimotty PA, Massobrio M, Regnani G, et al. Intratumoral T cells, recurrence and survival in epithelial ovarian cancer. N Engl J Med 2003; 348:203-13.
11. Galon J, Costes A, Sanchez-Cabo F, Kirilovsky A, Mlecnik B, Lagorce-Pages C, et al. Type, density and location of immune cells within human colorectal tumors predict clinical outcome. Science 2006; 313:1960-4.
12. Bach JF. Regulatory T cells under scrutiny. Nat Rev Immunol 2003; 3:189-98.
13. Shevach EM. $CD4^+$ $CD25^+$ suppressor T cells: more questions than answers. Nat Rev Immunol 2002; 2:389-400.
14. Zou W. Regulatory T cells, tumour immunity and immunotherapy. Nat Rev Immunol 2006; 6:295-307.
15. Rudensky AY, Gavin M, Zheng Y. FOXP3 and NFAT: partners in tolerance. Cell 2006; 126:253-6.
16. Wan YY, Flavell RA. Regulatory T-cell functions are subverted and converted owing to attenuated Foxp3 expression. Nature 2007; 445:766-70.
17. Ormandy LA, Hillemann T, Wedemeyer H, Manns MP, Greten TF, Korangy F. Increased populations of regulatory T cells in peripheral blood of patients with hepatocellular carcinoma. Cancer Res 2005; 65:2457-64.
18. Ichihara F, Kono K, Takahashi A, Kawaida H, Sugai H, Fujii H. Increased populations of regulatory T cells in peripheral blood and tumor-infiltrating lymphocytes in patients with gastric and esophageal cancers. Clin Cancer Res 2003; 9:4404-8.
19. Curiel TJ, Coukos G, Zou L, Alvarez X, Cheng P, Mottram P, et al. Specific recruitment of regulatory T cells in ovarian carcinoma fosters immune privilege and predicts reduced survival. Nat Med 2004; 10:942-9.
20. Petersen RP, Campa MJ, Sperlazza J, Conlon D, Joshi MB, Harpole DH, et al. Tumor infiltrating $Foxp3^+$ regulatory T-cells are associated with recurrence in pathologic stage I NSCLC patients. Cancer 2006; 107:2866-72.
21. Shimizu J, Yamazaki S, Sakaguchi S. Induction of tumor immunity by removing $CD25^+CD4^+$ T cells: a common basis between tumor immunity and autoimmunity. J Immunol 1999; 163:5211-8.
22. Siddiqui SA, Frigola X, Bonne-Annee S, Mercader M, Kuntz SM, Krambeck AE, et al. Tumor-infiltrating $Foxp3^-CD4^+CD25^+$ T cells predict poor survival in renal cell carcinoma. Clin Cancer Res 2007; 13:2075-81.
23. Walker MR, Kasprowicz DJ, Gersuk VH, Benard A, Van Landeghen M, Buckner JH, et al. Induction of FoxP3 and acquisition of T regulatory activity by stimulated human $CD4^+CD25^-$ T cells. J Clin Invest 2003; 112:1437-43.
24. Roncador G, Brown PJ, Maestre L, Hue S, Martinez-Torrecuadrada JL, Ling KL, et al. Analysis of FOXP3 protein expression in human $CD4^+CD25^+$ regulatory T cells at the single-cell level. Eur J Immunol 2005; 35:1681-91.
25. Ziegler SF. FOXP3: not just for regulatory T cells anymore. Eur J Immunol 2007; 37:21-3.
26. Curiel TJ. Regulatory T-cell development: is Foxp3 the decider? Nat Med 2007; 13:250-3.
27. Curiel TJ. Regulatory T cells and treatment of cancer. Curr Opin Immunol 2008; 20:241-6.
28. Taylor CR, Levenson RM. Quantification of immunohistochemistry—issues concerning methods, utility and semiquantitative assessment II. Histopathology 2006; 49:411-24.
29. Bock C, Paulsen M, Tierling S, Mikeska T, Lengauer T, Walter J. CpG island methylation in human lymphocytes is highly correlated with DNA sequence, repeats and predicted DNA structure. PLoS Genet 2006; 2:26.
30. Straussman R, Nejman D, Roberts D, Steinfeld I, Blum B, Benvenisty N, et al. Developmental programming of CpG island methylation profiles in the human genome. Nat Struct Mol Biol 2009; 16:564-71.
31. Olek A, Oswald J, Walter J. A modified and improved method for bisulphite based cytosine methylation analysis. Nucleic Acids Res 1996; 24:5064-6.
32. Rapko S, Baron U, Hoffmuller U, Model F, Wolfe L, Olek S. DNA methylation analysis as novel tool for quality control in regenerative medicine. Tissue Eng 2007; 13:2271-80.
33. Baron U, Turbachova I, Hellwag A, Eckhardt F, Berlin K, Hoffmuller U, et al. DNA methylation analysis as a tool for cell typing. Epigenetics 2006; 1:55-60.
34. Baron U, Floess S, Wieczorek G, Baumann K, Grutzkau A, Dong J, et al. DNA demethylation in the human FOXP3 locus discriminates regulatory T cells from activated FOXP3(+) conventional T cells. Eur J Immunol 2007; 37:2378-89.
35. Stockis J, Fink W, Francois V, Connerotte T, de Smet C, Knoops L, et al. Comparison of stable human Treg and Th clones by transcriptional profiling. Eur J Immunol 2009; 39:869-82.
36. Lewin J, Schmitt AO, Adorjan P, Hildmann T, Piepenbrock C. Quantitative DNA methylation analysis based on four-dye trace data from direct sequencing of PCR amplificates. Bioinformatics 2004; 20:3005-12.
37. Rasmussen R. Quantification on the LightCycler. In: Meuer S, Wittwer C, Nakagawara K, Eds. Rapid cycle real-time PCR, methods and applications. Edition Heidelberg: Springer Press 2001; 21-34.
38. Kaplan EL, Meier P. Nonparametric estimation for incomplete observations. J Am Statistic Ass 1958; 53:457-63.
39. Mantel N. Evaluation of survival data and two new rank order statistics arising in its consideration. Cancer Chem Rep 1966; 50:163-70.
40. Wieczorek G, Asemissen A, Model F, Turbachova I, Floess S, Liebenberg V, et al. Quantitative DNA methylation analysis of FOXP3 as a new method for counting regulatory T cells in peripheral blood and solid tissue. Cancer Res 2009; 69:599-608.
41. Pages F, Kirilovsky A, Mlecnik B, Asslaber M, Tosolini M, Bindea G, et al. In situ cytotoxic and memory T cells predict outcome in patients with early-stage colorectal cancer. J Clin Oncol 2009; 27:5944-51.
42. Galon J, Fridman WH, Pages F. The adaptive immunologic microenvironment in colorectal cancer: a novel perspective. Cancer Res 2007; 67:1883-6.